

Nanotechnology, Nanostructures, Nanomaterials

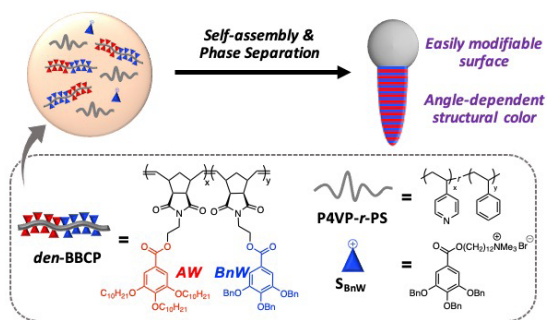
Multifunctional Photonic Janus Particles	87
Maskless Fourier Transform Holography Using Structured Light.....	88
Impact of 2D-3D Heterointerface on Remote Epitaxial Interaction through Graphene.....	89
Scale Two-dimensional Perovskite with Unity Photoluminescence Quantum Yield	90
Scalable Microfabrication of Microtextured Omniphobic Surface	91
Exciton-phonon Coupling in 2D Silver Phenyl Selenolate Revealed by Impulsive Vibrational Spectroscopy.....	92
Interface Energies of Metallic Nanoislands on Suspended 2D Materials.....	93
Robotic Synthesis and Testing of Nanocatalysts	94
Wet-based Digital Etching for High Aspect-ratio GaN Vertical Nanostructures.....	95
Chip-less Wireless Electronic Skins Enabled by Epitaxial Freestanding Compound Semiconductors	96
Fully 3D-Printed Electronics via Multi-Material Microsputtering	97
Implosion Fabrication of Vacant Structures for Nanophotonic Applications.....	98
3D Nanofabrication of Multi-materials by Diversified Fluorescent Microprinting and Volumetric Deposition.....	99
Controlled Synthesis of Large 2D Ultrathin SnSe Crystals with In-plane Ferroelectricity	100
Low-temperature Synthesis of Monolayer MoS ₂ on 200-mm Silicon Platform	101
Carbon Nanotube Nano-contacts for MoS ₂ Transistors	102

Multifunctional Photonic Janus Particles

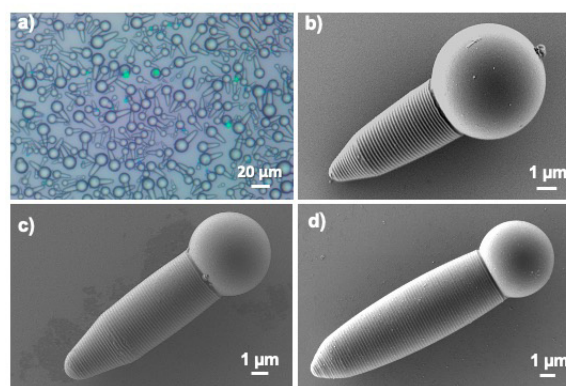
Q. He, H. Vijayamohan, J. Li, T. M. Swager
Sponsorship: Vannevar Bush Faculty Fellowship

Photonic Janus particles with a sphere fused to a cone are created from the phase separation of dendronized brush block copolymers (den-BBCP) and poly(4-vinylpyridine)-*r*-polystyrene (P4VP-*r*-PS) during the solvent evaporation of oil-in-water emulsions. Rapid self-assembly of den-BBCP generates well-ordered lamellar structures stacking along the long axis of the particles, producing structural colors that are dependent on the incident light angle. The colors are tunable over the visible spectrum by varying the molecular weight of den-BBCP. The P4VP-*r*-PS phase can undergo further surface modifications to produce multifunc-

tional photonic Janus particles. Specifically, a real-time magnetic control of the reflected color is achieved by coating the P4VP-*r*-PS phase with citric acid-capped Fe₃O₄ nanoparticles. Charged biomolecules (i.e., antibodies) are electrostatically immobilized to the Fe₃O₄ coating for potential applications in biosensing. As a demonstration, we developed a new photonic sensor for the foodborne pathogen *Salmonella* with antibody-modified photonic Janus particles, where the angle-dependent structural color plays a key role in the sensing mechanism.



▲ Figure 1: Preparation of photonic Janus particles by the phase separation of den-BBCP and P4VP-*r*-PS by the solvent evaporation of dichloromethane emulsions. Self-assembly of den-BBCP produces well-ordered multilayers to produce structural color. The surface of P4VP-*r*-PS phase can undergo further functionalization.



▲ Figure 2: Reflected light microscopy and scanning electron microscopy images of photonic Janus particles prepared with different den-BBCP₅₀₀ ($M_n = 500$ kDa) to P4VP-*r*-PS mass ratios: (a, b) 1:2, (c) 1:1, and (d) 2:1.

FURTHER READING

- Q. He, H. Vijayamohan, J. Li, and T. M. Swager, "Multifunctional Photonic Janus Particles," *J. Am. Chem. Soc.*, vol.144, no. 12, pp. 5661–5667, 2022.

Maskless Fourier Transform Holography Using Structured Light

K. Keskinbora, A. L. Levitan, Y. Yu, R. Comin

Sponsorship: German Research Foundation, Department of Energy

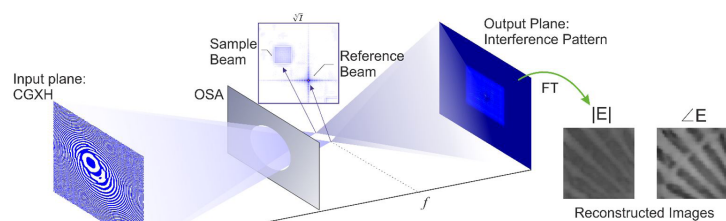
X-ray microscopy emerged as an ideal imaging tool for investigating nanoscale materials and devices with high spatio-temporal resolution. Visualizing the complex textures that underlie the macroscopic behavior of these systems will inform future device design. Advances in the wide availability of powerful graphical processors and high coherence X-ray sources lead to the emergence of new computational coherent imaging methods. However, these coherent imaging methods have many strings attached: some, such as ptychography, are incompatible with ultrafast imaging. Others, such as Fourier transform holography (FTH), which can be used for single-shot ultrafast imaging, are usually limited to preselected regions of interest. This severely limits the applicability of this method to magnetic films with homogeneous textures.

We aimed to develop a new X-ray holographic microscopy method without these limitations for investigating quantum electronic and magnetic solids at the nanoscale. Our technique relies on an X-ray wavefront shaping computer-generated hologram (CGH) to split the incident radiation into reference and sample beams. The reference beam propagates freely while the sample beam traverses the sample and is imprinted with phase information that encodes the sample's internal electronic and magnetic textures, as depicted schematically in Figure 1. A detector then captures the far-field interference pattern

from which the sample exit wave is recovered with nanometer spatial resolution. This exit wave reveals the samples' composition, density, and magnetization state. Our approach has several advantages over the conventional FTH: (i) the sample and reference beams are not defined by pre-patterned structures, avoiding the time-consuming sample preparation; (ii) the field of view is not physically anchored to a preselected region, allowing investigation of extended samples; and (iii) the approach is compatible with single-shot, ultra-fast spatiotemporal imaging of dynamics at the nanoscale.

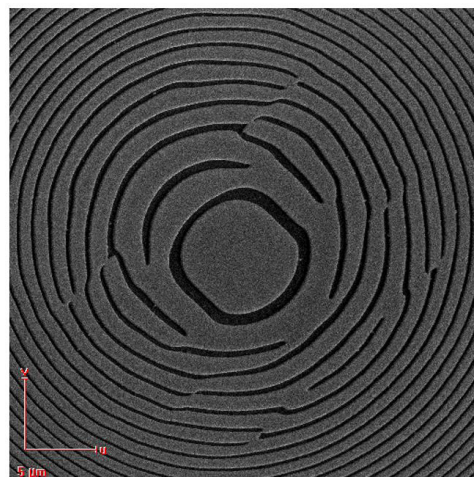
Critically, the method depends on the successful realization of a CGH, synthesized using a double-constraint Gerchberg-Saxton algorithm on MIT's Supercloud cluster. We have utilized a dedicated ion beam lithography tool at MIT.nano to transfer the computer-generated design into a gold-coated silicon nitride membrane with high fidelity to the design file. The resulting diffractive optic (see Figure 2) with a 300- μm aperture and 50-nm wide effective outermost zone width was successfully utilized in a recent experiment to demonstrate the first X-ray demonstration of the method. The results of those experiments are currently being analyzed.

Successful further development of the method can have far-reaching applications extending beyond hard condensed matter physics and the study of biological and soft matter through phase-contrast imaging.



▲ Figure 1: Overview of the experimental setup for a structured illumination X-ray holography experiment. The diffractive optics is the key to the successful realization of the method.

► Figure 2: A scanning electron microscope image of the central portion of a computer-generated hologram designed for soft X-rays and fabricated using VELION at MIT.nano.



FURTHER READING

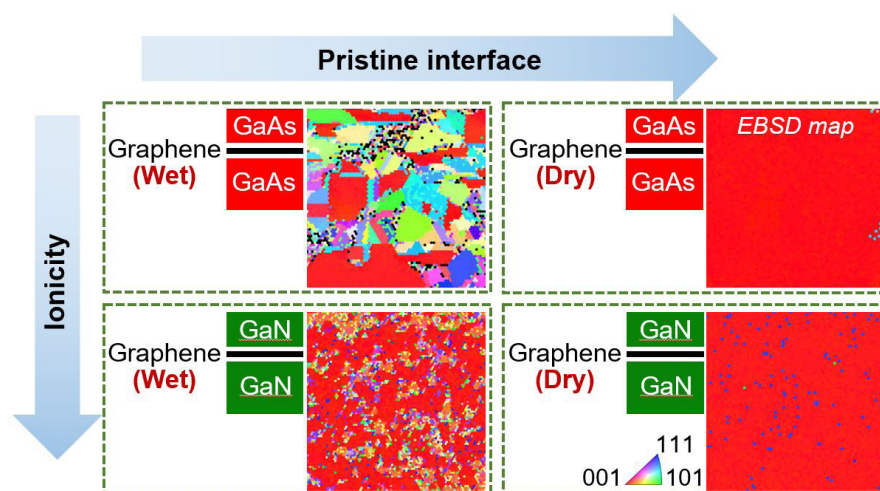
- K. Keskinbora, A. L. Levitan, and R. Comin, "Maskless Fourier Transform Holography," *Opt. Express*, vol. 30, pp. 403-413, 2022.

Impact of 2D-3D Heterointerface on Remote Epitaxial Interaction through Graphene

H. Kim, K. Lu, Y. Liu, H. S. Kum, K. S. Kim, K. Qiao, S. Lee, C. Choi, J. Kim
Sponsorship: DARPA, Department of Energy, U.S. Air Force Research Laboratory

Remote epitaxy has drawn attention as it offers epitaxy of functional materials that can be released from the substrates with atomic precision, thus enabling production and heterointegration of flexible, transferrable, and stackable freestanding single-crystalline membranes. In addition, the remote interaction of atoms and adatoms through two-dimensional (2D) materials in remote epitaxy provides a platform to investigate and utilize electrical/chemical/physical coupling of bulk (3D) materials via 2D materials (3D-2D-3D coupling). Here, we unveil the respective roles and impacts of the substrate material, graphene, substrate-graphene interface, and epitaxial material for electrostatic coupling of these materials, which governs cohesive ordering and can lead to single-crystal epitaxy in the overlying film.

We show that simply coating a graphene layer on wafers does not guarantee successful implementation of remote epitaxy, since atomically precise control of the graphene-coated interface is required, and provide key considerations for maximizing the remote electrostatic interaction between the substrate and adatoms. The experimental study is conducted by exploring various material systems and processing conditions, and we demonstrate that the rules of remote epitaxy vary significantly depending on the ionicity of material systems as well as the graphene-substrate interface and the epitaxy environment. The general rule of thumb discovered provides a cornerstone for expanding 3D material libraries that can be stacked in freestanding form to revolutionize heterogeneous integration.



▲ Figure 1: Electron backscatter diffraction (EBSD) maps show better crystal quality in remote epitaxial films when the interface is pristine and the materials have high ionicity.

FURTHER READING

- D. MacNeill, J. T. Hou, D. R. Klein, P. Zhang, P. Jarillo-Herrero, and L. Liu, *Physical Review Letters*, vol. 123, p. 047204, 2019.

Scale Two-dimensional Perovskite with Unity Photoluminescence Quantum Yield

D. Lee, K. Kim, Y. Li, Y. Yu, B. Xu, J. Kim

Sponsorship: Southern University of Science and Technology

Two-dimensional (2D) materials with high photoluminescence quantum yield (PLQY) and broad ranges of bandgap are essential for high performance 2D optoelectronic applications. Even though transition metal dichalcogenides (TMDCs) have been mainstream in 2D material community, their bandgap ranges from 1.5eV to 2eV and cannot cover wide bandgap applications above 2.0eV. In addition, the best PLQY value has been ~95% with chemically doped MoS₂, and its lateral dimension has been limited to hundreds of micrometers.

In this regard, 2D organic-inorganic hybrid perovskite (PVSK) has been studied extensively because of its tunable band gap up to 3eV by adjusting

organic cations and halide anions. However, achieving high PLQY and isolating bulk 2D PVSK crystal into monolayers in centimeter scale are still challenging.

In this work, we successfully synthesized high-quality single-crystalline 2D PVSK with the world's best PLQY (~99.3%) and isolated them into atomic-scale thickness via a layer-resolved splitting (LRS) process. With the astonishing achievements, the tunable bandgap of 2D PVSK up to 3eV will expand the applications of 2D materials, and device performance would be further improved thanks to its unity PLQY.

Scalable Microfabrication of Microtextured Omniphobic Surface

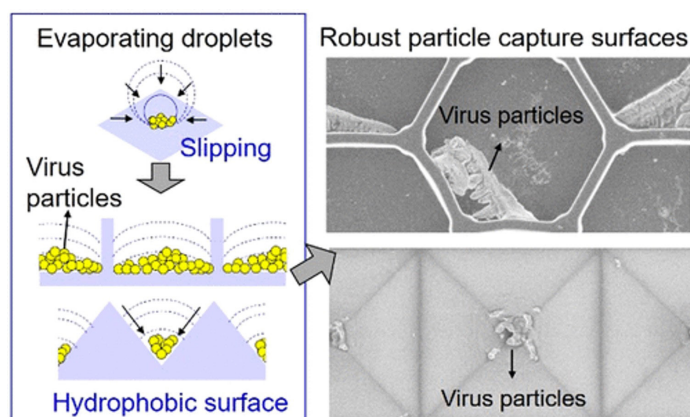
S. Kim, S.-H. Nam, Y. T. Cho, N. X. Fang

Sponsorship: Ministry of Trade, Industry & Energy (MOTIE, Korea), National Research Foundation (NRF) of Korea

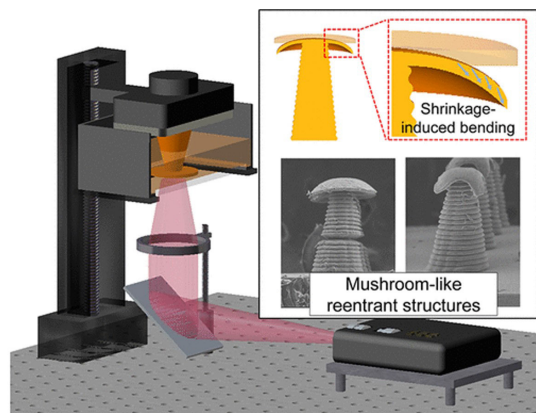
In this joint research between Changwon National University (Korea) and the Fang group at MIT, we explore scalable microfabrication of 2D patterns and 3D shapes—and arrangements of those patterns into different shapes—with potential to control surface wetting and adhesion by tailored microtextures. One of the interesting phenomena is the “rose petal” effect, in which a hydrophilic material macroscopically behaves in a hydrophobic manner if its surface contains the suitable microstructural features. This Rose petal effect produces an effective design for self-cleaning, anti-sticking, oil/water separation, microreactors, and droplet manipulation. As an example, particle aggregation was directionally controlled using contact line dynamics (pinned or slipping) and geometrical gradients on microstructured surfaces by the systematic investigation of the evaporation process on sessile droplets and sprayed microdroplets laden with virus-simulant nanoparticles. We demonstrated the potentials of an

engineered microcavity surface to limit the contact transfer of particle aggregates deposited with the evaporation of microdroplets by 93% for hexagonal microwalls and by 96% for inverted pyramidal microwalls. The particle capture potential of the interconnected microstructures was also investigated using biological particles, including adenoviruses and lung-derived extracellular vesicles.

As a continuation of this work, we aim to (1) develop micro-nano surface engineering based on the imprint process and additive manufacturing; (2) fabricate and characterize practical devices for implementing a bio-inspired functional surface (see Figures 1 and 2 from Fang et al.); and (3) employ a prototype in biological, health, energy, and environmental applications. The successful implementation of this work will present effective and practical ways to improve public health and personal hygiene.



▲ Figure 1: Robust particle capture surfaces via ultraviolet imprint.



▲ Figure 2: 3D printed shape-deformed microstructure exhibits a liquid repellency without perfluorinated coating.

FURTHER READING

- S. Kim, W. Y. Kim, S.-H. Nam, S. Shin, S. H. Choi, D. H. Kim, H. Lee, H. J. Choi, E. Lee, J.-H. Park, I. Jo, N. X. Fang, and Y. T. Cho et al., “Microstructured Surfaces for Reducing Chances of Fomite Transmission via Virus-Containing Respiratory Droplets,” *ACS Nano*, vol. 15, no. 9, pp. 14049-14060, August 2021, <https://doi.org/10.1021/acsnano.1c01636>.
- D. H. Kim, S. Kim, S. R. Park, N. X. Fang, and Y. T. Cho et al., “Shape-Deformed Mushroom-like Reentrant Structures for Robust Liquid-Repellent Surfaces,” *ACS Appl. Mater. Interfaces*, vol. 13, pp. 33618-33626, July 2021, <https://doi.org/10.1021/acscami.1c06286>.

Exciton-phonon Coupling in 2D Silver Phenyl Selenolate Revealed by Impulsive Vibrational Spectroscopy

E. R. Powers*, W. Paritmongkol*, D. C. Yost, W. S. Lee, J. C. Grossman, W. A. Tisdale

*Authors contributed equally

Sponsorship: National Defense Science and Engineering Graduate Fellowship

Semiconductor nanomaterials have the potential to be employed in next-generation optoelectronic devices that exhibit significantly improved performance at reduced cost. Two-dimensional metal-organic chalcogenolates (MOCs) are a newly discovered class of nanomaterials that combine many of the best properties of TMDs transition metal dichalcogenides and 2D perovskites, two more established 2D semiconductor families. Silver phenyl selenolate (AgSePh) is the prototypical example, a hybrid organic-inorganic material comprised of 2D sheets that exhibit a narrow bandwidth 467-nm blue emission and 2D in-plane exciton anisotropy. Additionally, crystalline AgSePh is easy to synthesize and stable under ambient conditions. Owing to these advantages, MOCs may be useful in applications like light-emitting diodes or photodetectors.

While early studies are promising, the underlying physics of AgSePh has not been fully explored. In this work, we employ impulsive vibrational spectroscopy (IVS) to investigate the degree of exciton-phonon coupling in AgSePh. Using this time-domain Raman method, we resolve multiple coherent vibrational signatures, suggesting strong exciton-phonon coupling in this material. Molecular dynamics (MD) and density functional theory simulations are also performed to calculate a phonon density of states

for AgSePh. A comparison of experimental and simulation results allows us to visualize the structural displacements that occur as a result of the vibrational modes identified with IVS. From these data, we make conclusions about why certain vibrational modes are electronically coupled while others are not.

These results are also compared to low frequency Raman and temperature-dependent photoluminescence data, corroborating the previous findings and improving our understanding of the vibrational landscape of the AgSePh system. Finally, temperature-dependent IVS studies of the vibrational mode frequencies and lifetimes are performed from 5K to 300K, revealing information about mode anharmonicity and phonon scattering processes.

These results present a convincing picture of strong electronic-vibrational interactions in 2D hybrid AgSePh. Our work provides insight into the underlying structural and electronic properties of AgSePh and other MOCs, which will help to inform future development of new structures and syntheses that can control exciton-phonon coupling and further expand the capabilities and applications of this new material family.

FURTHER READING

- W. Paritmongkol, T. Sakurada, W. S. Lee, R. Wan, P. Muller, and W. A. Tisdale, "Size and Quality Enhancement of 2D Semiconducting Metal-Organic Chalcogenolates by Amine Addition," *Journal of the American Chemical Society*, vol. 143, pp. 20256-20263, Nov. 2021.

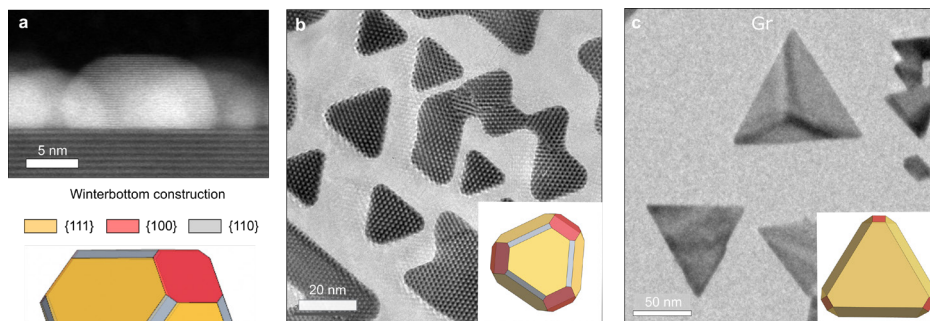
Interface Energies of Metallic Nanoislands on Suspended 2D Materials

K. Reidy, J. D. Thomsen, B. Wang, F. M. Ross
Sponsorship: MIT Energy Initiative, Mathworks Engineering

A thorough understanding of the processing and properties of metal deposition on two-dimensional (2D) materials is crucial for tailoring the performance of solid-state devices that incorporate 2D materials. For example, the kinetics of metal deposition on 2D materials, including nucleation, epitaxy, and morphology, strongly influences 2D/3D device properties such as contact resistance, optical response, and high-frequency electrical performance. In particular, the interface energy between the metal and 2D material is an important parameter which determines the nanoislands' shape and resulting catalytic properties, plasmonic behavior, and excitonic coupling of the heterostructure.

Here, we determine the interface energies of single crystalline Au nanoislands with well-defined faceted morphologies grown epitaxially on suspended 2D materials. Focusing initially on Au deposited on MoS₂, we investigate quasi-van der Waals epitaxial growth of compact Au triangles ~20 nm in lateral size, flat topped, and 4-8 nm tall (Figures 1a,b). These nanoisland shapes

are consistent with the equilibrium Winterbottom shape of Au on MoS₂, which is bounded by {111}, {110}, and {100} facets. A combination of cross-sectional and plan view transmission electron microscopy (TEM) imaging shown in Figures 1a,b allows us to measure the nanoislands' shape in three dimensions and estimate an interface energy of MoS₂/Au as 0.14-0.18 J/m² through thermodynamic modelling. We then compare these results to Au deposited on graphene, which exhibits more pointed corners due to an Au{111} surface reconstruction (Figure 1c). This leads to a Gr/Au interface energy of ~ 0.07 – 0.14 J/m², slightly lower than that calculated for the MoS₂/Au system. This difference may be expected due to the difference in strength between Au-C vs. Au-S bonding. The structure and energetics of these quasi-van der Waals interfaces will open opportunities for novel mixed dimensional 2D/3D nanodevices and improve metal integration in current 2D devices.



▲ Figure 1: a) Atomic resolution cross-sectional scanning TEM image showing MoS₂/Au island shape (top) and side view of corresponding Winterbottom construction (bottom). b) Plan-view TEM of triangular Au nanoislands on clean suspended MoS₂. Inset show theoretical Winterbottom construction. c) Plan-view TEM of triangular Au nanoislands on clean suspended Gr. Inset show theoretical Winterbottom construction with Au(111) surface energy reduction by 0.15 J/m² to account for surface reconstruction

FURTHER READING

- K. Reidy*, G. Varnavides*, J. D. Thomsen, A. Kumar, T. Pham, A. M. Blackburn, P. Anikeeva, P. Narang, J. M. LeBeau, and F. M. Ross, "Direct Imaging and Electronic Structure Modulation of Moiré Superlattices at the 2D/3D Interface," *Nat Comm.*, vol. 12, p. 1290, 2021.
- K. Reidy, J. D. Thomsen, H. Y. Lee, V. Zarubin, Y. Yu, B. Wang, T. Pham, and F. M. Ross, "Quasi-van der Waals Epitaxy of 3D Metallic Nanoislands on Suspended 2D Materials," 2022.

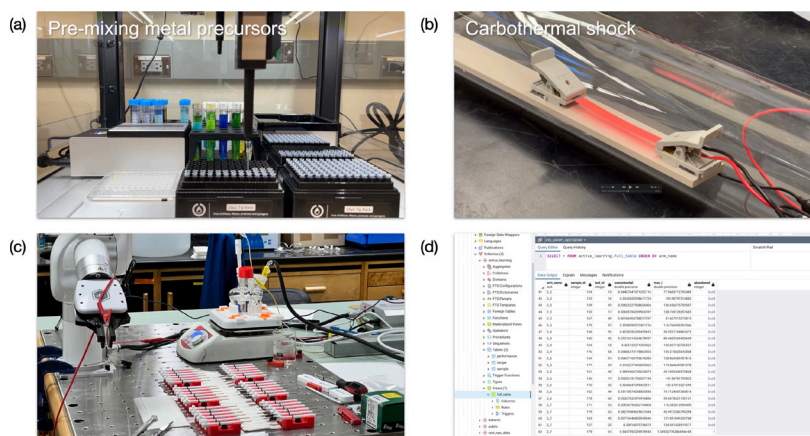
Robotic Synthesis and Testing of Nanocatalysts

Z. Ren, A. Abdelhafiz, Z. Zhang, J. Li
Sponsorship: Honda Research Institute USA

Research solutions aiming to replace existing hydrocarbon fuel technologies with green energy sources have only partially succeeded. Proton-exchange membrane fuel cells (PEMFC) are a very promising candidate for their light weight and high energy density, while catalysts used in the cell electrode limit its performance and durability. Recent studies show that synergistic effects of multiple metals alloyed together yield a material even better than noble metal catalysts. Yet such a very well controlled and precise synthesis of more than tri-metallic nanoparticles is extremely challenging by conventional synthesis techniques at normal/ambient conditions, which thermodynamic rules dictate. Ultrafast Joule heating technique is a promising tool to leverage kinetic rules to form meta-stable high entropy alloys by heating and cooling samples within one second. This extremely fast process makes it practical to make the workflow in a high-throughput manner.

The high throughput system consists of a liquid handler, a carbothermal shock setup, and a robotic testing platform. The liquid handling robot allows us to precisely control the composition of each sample,

specifically, the ratio between each metal precursor solution (Figure 1a). Carbothermal shock (Figure 1b) is enabled by conducting a large current (>10 A) to a precursor loaded carbon substrate, which can reach above 2000 K within hundreds of milliseconds. Once the carbon strips are prepared via shocking, a rapid evaluation will be conducted, also in a high-throughput manner. Samples will be cut into pieces and loaded onto testing holders; a robotic arm will load and unload samples to the electrocatalytic testing beaker. Testing software is automated using python scripts, data extraction, and a structured query language (SQL) storage process (Figure 1d). Finally, an active learning step analyzes the dataset using Bayesian optimization to generate the suggestion for the next batch of recipes, based on the surrogate model fitted by the Gaussian process. The newly suggested task will be sent to the liquid handler in Figure 1a, forming a closed-feedback optimization loop. Such a high-throughput and autonomous optimization system will greatly enhance the efficiency of finding new high entropy alloy recipes for electrocatalyst application.



▲ Figure (1a) Liquid handler capable of preparing 72 samples in a batch, (1b) carbothermal shock process that can transform metal precursor to high-entropy alloys within 1 sec, (1c) robotic testing capable of evaluating 36 samples in a batch, (1d) dataset stored on a SQL server that can be read by active learning algorithm.

FURTHER READING

- Z. Ren, "Robotic Synthesis and Testing of Nanocatalysts" [Online]. Available: https://youtu.be/WOQj_EJekoo (Apr. 2022).
- Z. Ren, "Liquid Handling Robot with 3D Printed Pipette Handler," [Online]. Available: <https://youtu.be/ScDYSUFREZo> (Sept. 2020).
- K. Li, and W. Chen. "Recent Progress in High-entropy Alloys for Catalysts: Synthesis, Applications, and Prospects." *Materials Today Energy*, vol. 20, pp. 100638, Jun. 2021.

Wet-based Digital Etching for High Aspect-ratio GaN Vertical Nanostructures

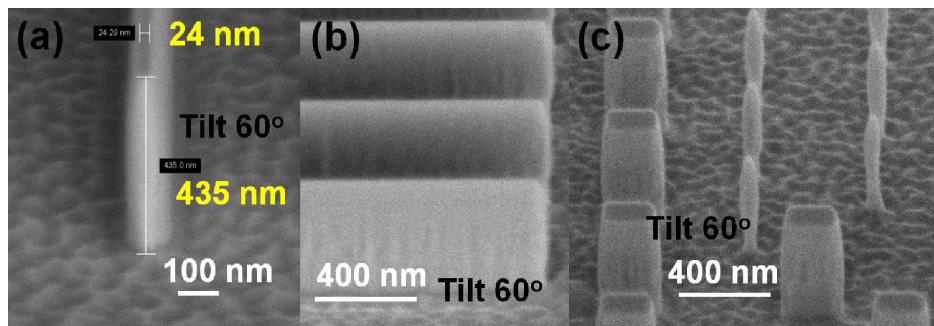
P.-C. Shih, T. Palacios, in collaboration with G. Rughoobur, A. I. Akinwande

Sponsorship: U.S. Air Force Office of Scientific Research through MURI Empty State Electronics Project

III-Nitrides have been studied and used for high-frequency and power electronics thanks to their excellent material properties. However, there are still challenges for their use in some applications, such as micro-light-emitting diodes, field emitters, and other vertical devices. Traditionally, high-aspect-ratio III-Nitride nanostructures are fabricated by two-step etchings combining (1) plasma dry etching and (2) wet-chemical orientation-dependent etching. Heated tetramethylammonium hydroxide (TMAH) or KOH-based chemicals are usually used for obtaining vertical sidewalls; however, the process yield and variation can be difficult to control due to defects in materials and plasma damage.

GaN vertical sidewalls formed by dry etching have been demonstrated in literature; however,

demonstrations of sub-50-nm high-aspect-ratio nanostructures are still limited. In this work, a wet-based digital etching technology is combined with an optimized plasma dry etching for high-aspect-ratio GaN vertical fins and nanowires (NWs). The vertical sidewalls of GaN vertical structures can be obtained by the optimized dry etching, and the width of these vertical structures can be shrunk by the subsequent wet-based digital etching. Vertical fin and NW arrays with sub-40-nm width and a $> 10:1$ aspect ratio are demonstrated with good uniformity and reproducibility (Figure 1). These developed technologies can be applied for different devices, such as vertical power fin field-effect transistors (FinFETs), NW FETs, micro-LEDs, and lateral FinFETs, with sub-50-nm dimensions and high aspect ratios in the future.



▲ Figure 1: Tilted scanning electron microscope (SEM) images of (a) a GaN vertical fin, (b) fins' sidewalls, and (c) GaN nanowires with $>10:1$ aspect-ratio after digital etching. The aspect ratio of GaN fin can be close to $20:1$ with this approach.

FURTHER READING

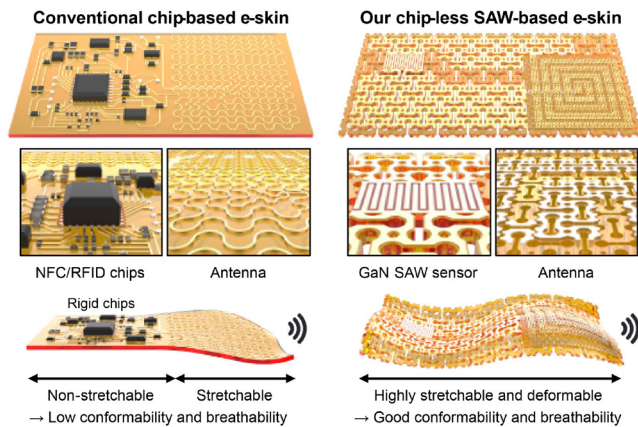
- P.-C. Shih, G. Rughoobur, K. Cheng, A. I. Akinwande, and T. Palacios, "Self-Align-Gated GaN Field Emitter Arrays Sharpened by a Digital Etching Process," *IEEE Electron Device Letters*, vol. 42, no. 3, pp. 422-425, Mar. 2021.
- P.-C. Shih, Z. Engel, H. Ahmad, W. A. Doolittle, and T. Palacios, "Wet-based Digital Etching on GaN and AlGaN," *Applied Physics Letters*, vol. 120, p. 022101, 2022.

Chip-less Wireless Electronic Skins Enabled by Epitaxial Freestanding Compound Semiconductors

Y. Kim, J. M. Suh, Y. Liu, J. Shin, J. Kim
Sponsorship: Amore Pacific

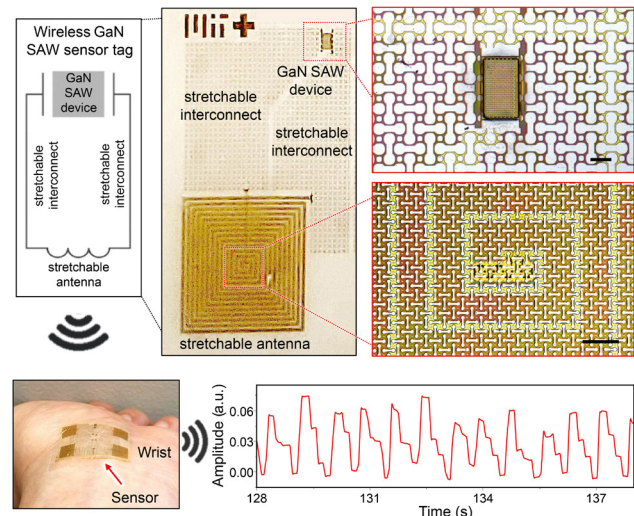
Electronic skin (e-skin) has been developed with a goal to obtain a non-invasive human health monitoring electronic system with its imperceptibility. So far, one of the major shortcomings in this field is the bulky wireless communication system that severely affects its wearability (Figure 1). In this paper, we introduce a single-crystalline non-Si-based e-skin system where fully conformable, ultrathin, piezoelectric, compound semiconductor membranes are incorporated as power-efficient wireless communication modules and extremely high sensitivity sensors without needing for bulky chips and batteries. The developed GaN surface

acoustic wave-based device successfully measured wirelessly three different inputs including strain, ultra-violet light, and ion concentrations (Figure 2). The consistency and accuracy of the measured heart rate and pulse waveforms over a 7-day period, during which the e-skin was re-attached 7 times, strongly demonstrate the reusability and long-term wearability of our device. This study will change the paradigm of e-skins by providing versatile wireless platforms for fully imperceptible e-skins with very high sensitivity and low power consumption.



◀ Figure 1: Comparison between (left) conventional wireless e-skin based on integrated circuit chips and (right) our chip-less wireless e-skin based on surface acoustic wave (SAW) devices made of GaN freestanding membranes.

▶ Figure 2: Schematic and optical images of our wireless GaN SAW e-skin strain sensor and wireless pulse measurements using our GaN SAW e-skin strain sensors. Scale bars indicate 200 μm .



FURTHER READING

- H. Yeon, H. Lee, Y. Kim, D. Lee, Y. Lee, J.-S. Lee, J. Shin, C. Choi, et al., "Long-term Reliable Physical Health Monitoring by Sweat Pore-inspired Perforated Electronic Skins," *Sci. Adv.*, vol. 7, no. 27, eabg.8459, Jun. 2021.
- Y. Kim, S. S. Cruz, K. Lee, B. O. Alawode, C. Choi, Y. Song, J. M. Johnson, C. Heidelberger, et al., "Remote Epitaxy Through Graphene Enables Two-Dimensional Material-based Layer Transfer," *Nature*, vol. 544, pp. 340-343, Apr. 2017.
- H. S. Kum, H. Lee, S. Kim, S. Lindemann, W. Kong, K. Qiao, P. Chen, J. Irwin, et al., "Heterogeneous Integration of Single Crystalline Complex-oxide Membranes," *Nature*, vol. 578, pp. 75-81, Feb. 2020.

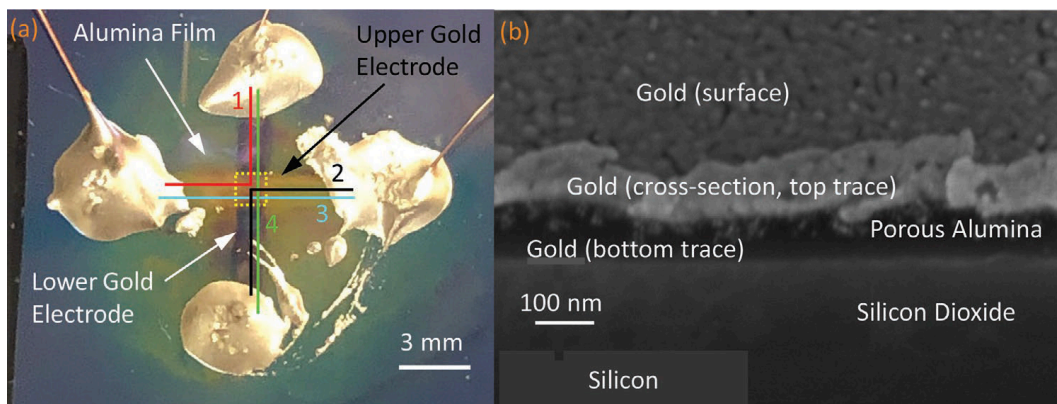
Fully 3D-Printed Electronics via Multi-Material Microsputtering

Y. S. Kornbluth, L. Parameswaran, R. Mathews, L. M. Racz, L. F. Velásquez-García
Sponsorship: Kansas City National Security Center

Integrated circuits (ICs) are made in multibillion-dollar foundries, involving extreme processing conditions. To attain low per-chip cost, many identical IC chips are batch processed. Lower volume electronics are manufactured at a low cost using printed circuit boards, where premade components, often made in a foundry, are soldered onto a dielectric plate with an arrangement of thin film conductive traces and a set of drilled vias. However, currently, there is no cost-effective approach to make a small batch of ICs, conduct chip-to-chip customization, or rework ICs.

In this project, we are harnessing microplasma sputtering (i.e., the sputtering of materials at atmospheric pressure using reactors with characteristic length below millimeters) to develop a manufacturing platform for agile manufacturing of ICs. We recently reported the first fully additively

manufactured capacitors as a proof-of-concept demonstration of such multi-material microplasma sputtering manufacturing platform. This is also the first demonstration of a cleanroom-quality, multi-material electrical device produced entirely through additive manufacturing. The conductive films are created by sputtering gold in air, attaining near-bulk electrical conductivity. The dielectric films are created by sputtering aluminum in a gas blend of argon and air, resulting in alumina films (Figure 1). The frequency response of the capacitor is described by the universal dielectric response typically found in heterogenous dielectrics and suggests the presence of condensed water in the pores of the alumina film. Future work could entail extending the platform to other transducing materials, e.g., semiconductors.



▲ Figure 1: (a) Photograph of a fully microsputtered capacitor composed of two perpendicular gold lines separated by a thin alumina film. (b) Scanning electron microscope (SEM) cross-section of microplasma-printed capacitor; the gold films are 50 nm thick, while the alumina film is 35 nm thick. From Y. Kornbluth et al., *Advanced Materials Technologies* (2022).

FURTHER READING

- Y. Kornbluth, R. H. Mathews, L. Parameswaran, L. Racz, and L. F. Velásquez-García, "Fully 3D-printed, Ultrathin Capacitors via Multi-material Microsputtering," *Advanced Materials Technologies*, to be published, 2022.
- Y. Kornbluth, R. H. Mathews, L. Parameswaran, L. Racz, and L. F. Velásquez-García, "Nano-additively Manufactured Gold Thin Films with High Adhesion and Near-bulk Electrical Resistivity via Jet-assisted, Nanoparticle-dominated, Room-temperature Microsputtering," *Additive Manufacturing*, vol. 36, p. 101679, Dec. 2020.
- Y. Kornbluth, R. H. Mathews, L. Parameswaran, L. Racz, and L. F. Velásquez-García, "Room-temperature, Atmospheric-pressure Deposition of Dense, Nanostructured Metal Films via Microsputtering," *Nanotechnology*, vol. 30, no. 28, p. 285602, Jul. 2019.

Implosion Fabrication of Vacant Structures for Nanophotonic Applications

Q. Yang†, G. Yang†, C. Zheng, T. Nambara, Y. Kunai, A. C. Matlock, H. Kusaka, D. Wadduwage, P. T. C. So, E. S. Boyden

†These authors contributed equally to this work.

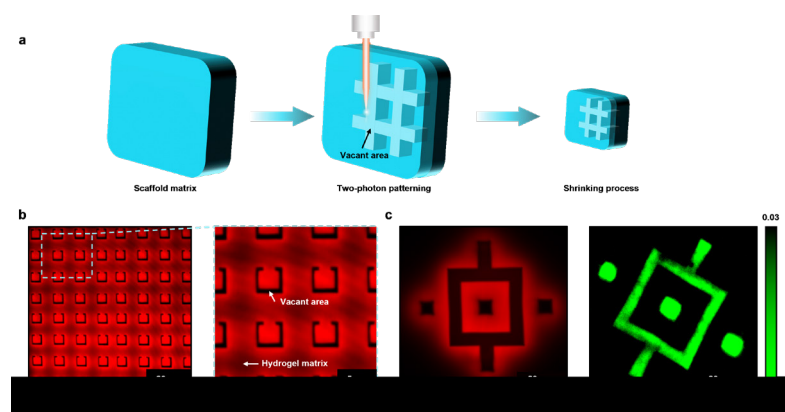
Sponsorship: Fujikura

Implosion fabrication (ImpFab) is an emerging nanofabrication strategy that allows complex free-form 3D architectures to be crafted with nanometer precision while being compatible with a wide range of organic and inorganic materials. In ImpFab, a hydrogel is photopatterned with a multiphoton laser, chemicals, and nanoparticles attached to the photopatterned sites; the sample is then shrunk to yield nanoprecise features. Such a method presents a strong potential for applications in nanophotonics, where the refractive index (RI) difference between a structure and its environment is critical. Volumetric deposition of high RI nanoparticles is a promising direction; conversely, volumetric ablation/removal to generate RI differences between the hydrogel matrix and inner vacant structures is another possible way.

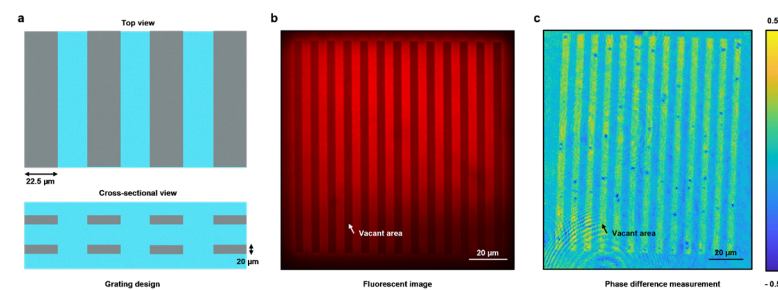
We have achieved high-resolution vacant structures appears in Figure 1a. The fabrication procedure begins with soaking the hydrogel scaffold matrix in dye solution, followed by the two-photon patterning and shrinking process, to generate high-

density and high-resolution vacant structures in the scaffold. The “C-type” vacant structure array in Figure 1b demonstrates the capability of ImpFab to achieve complex architectures for potential nanophotonic application. The RI difference is essential; measurement results by holotomography microscopy appear in Figure 1c. RI difference between the scaffold and the CaCl₂ solution is ~ 0.03 .

One promising photonic application of the proposed technology is an optical computing device. Such a device can achieve all-optical inference/prediction, which is considered much faster than traditional electron-based computing. To prove the concept, our first design appears in Figure 2a. The fluorescent image of the structure appears in Figure 2b. Tuning the thickness of each vacant structure can control the phase change. Figure 2c shows a grating structure with vacant structures at a thickness of $\sim 4.4 \mu\text{m}$, which presents a 0.3π phase change when measured.



◀ Figure 1: 3D vacant structures by ImpFab. a) ImpFab constructs vacant structures. b) Complex vacant structure array with nine-fold shrinkage. c) Holotomography microscopic measurement of the RI difference.



◀ Figure 2: Grating structures for optical computing devices. a) Top and cross-sectional views of grating designs. b) A fluorescent image of the grating pattern. c) Phase difference measurement presents $\sim 0.3 \pi$ change between the vacant structure and the scaffold.

FURTHER READING

- D. Oran, S. G. Rodriqus, R. Gao, S. Asano, M. A. Skylar-Scott, F. Chen, P. W. Tillberg, A. H. Marblestone, and E. S. Boyden, “3D Nanofabrication by Volumetric Deposition and Controlled Shrinkage of Patterned Scaffolds,” *Science*, vol. 362, pp. 1281-1285, Dec. 2018.

3D Nanofabrication of Multi-materials by Diversified Fluorescent Microprinting and Volumetric Deposition

G. Yang, Q. Yang, C. Zheng, D. Oran, E. S. Boyden

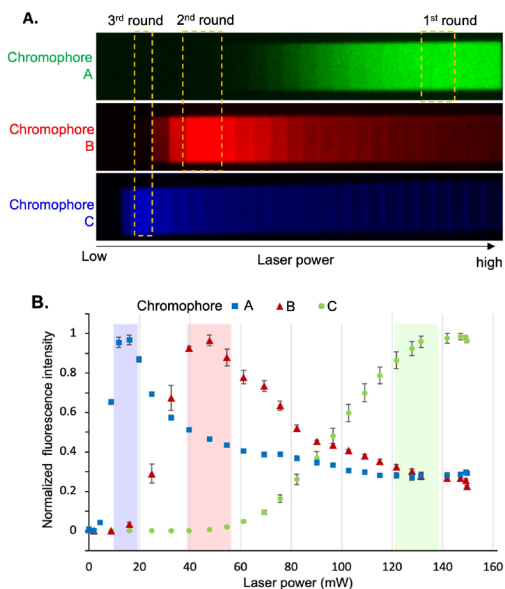
Sponsorship: Fujikura and International Relations and Security Network (ISN-5-PPA-02)

Multi-material (MM) 3D printing, which enables production of highly functional structures by integrating MMs, has attracted attention, and a variety of fabrication methods have been developed. Most 3D printing approaches so far, however, require complex equipment, and the printed structures are limited in accuracy and resolution. Unlike the conventional approaches, we developed an advanced MM 3D patterning method for high-speed and high-accuracy construction of nanoscale structures. By utilizing photo-activatable chromophores and varied multiphoton laser powers, we combine different chromophores into a polyacrylate hydrogel in predetermined locations and combinations. After selective deposition of different materials to the patterned chromophore regions, the hydrogel is linearly shrunk to generate an MM 3D nanostructure.

As Figure 1 shows, increasing laser intensity achieves three chromophores with different fluorescent profiles, making it feasible to selectively activate one chromophore at a time. After that, a 3D multi-pattern was generated, in the absence of a

complex microfluidic system or mechanical control. Moreover, this method could keep the sample static in the whole process and thus lead to high printing accuracy. Figure 2 demonstrates fabrication of an MM structure in a step-by-step manner. After the multi-patterning process, different molecules or nanoparticles were selectively deposited one by one. In this nanoscale “MIT” logo, each single letter was patterned with one chromophore and deposited with different materials: the letter “M” was filled with silver and gold, “I” with cadmium telluride, and “T” with carbon nanotubes. Next, we plan to fabricate 3D metastructures and electrical components in nanoscale (shown in Figure 3), which might be used for optical or optoelectronic devices.

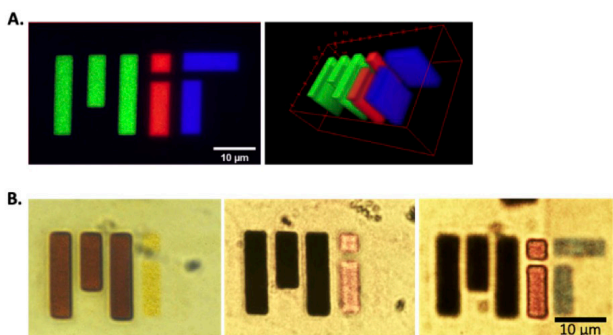
With regard to applications, we expect our new nanofabrication of MMs with complex, non-self-supporting 3D geometries to substantially broaden the applicability of nanoscale photonic devices, nanoelectronics, biosensors, diffractive optical elements, holograms, and multi-functional lenses.



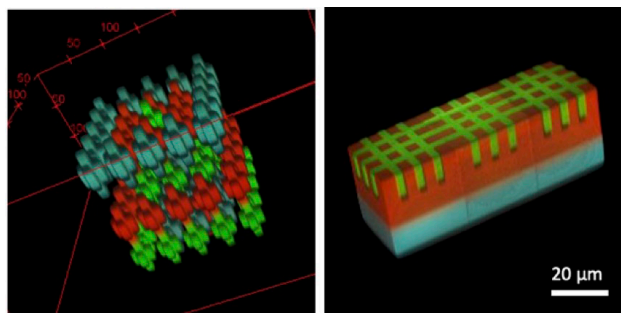
▲ Figure 1: A) Fluorescent images of linear gradient patterns of chromophores generated by varied two-photon laser power. B) Corresponding fluorescent intensity of patterned chromophores activated by varied laser power.

FURTHER READING

- D. Oran, S. G. Rodrigus, R. Gao, S. Asano, M. A. Skylar-Scott, F. Chen, P. W. Tillberg, A. H. Marblestone, and E. S. Boyden, “3D Nanofabrication by Volumetric Deposition and Controlled Shrinkage of Patterned Scaffolds,” *Science*, vol. 362, pp. 1281-1285, Dec. 2018.



▲ Figure 2: A) Fluorescent images of multi-patterned MIT logo; B) Bright field images of selective deposition of different materials in each step.



▲ Figure 3: Fluorescent images of 3D demos of metastructure (left) and electrical components (right).

Controlled Synthesis of Large 2D Ultrathin SnSe Crystals with In-plane Ferroelectricity

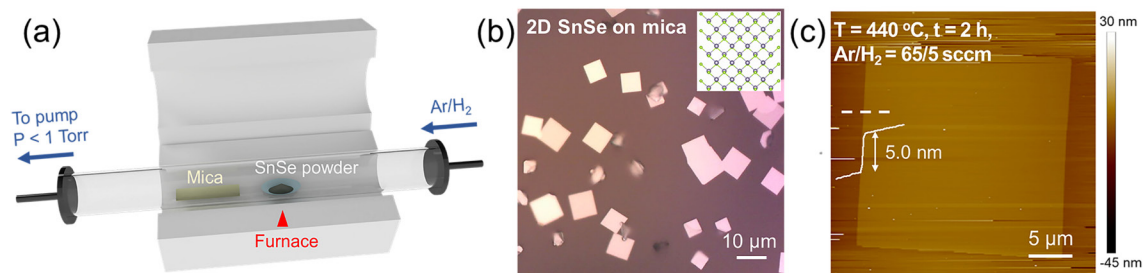
T. Zhang, M. Chiu, N. Mao, X. Ji, J. Kong

Sponsorship: Army Research Office MURI (W911NF-18-1-0432), NSF Science and Technology Center for Integrated Quantum Materials (DMR-1231319)

Tin selenide (SnSe) is an emerging member of two-dimensional (2D) layered materials with many intriguing properties, such as excellent thermoelectric performance, purely in-plane ferroelectricity, large piezoelectric coefficients, and strong non-linear optical responses. Moreover, as a semiconducting material that is structurally analogous to layered black phosphorus, a rising star for next-generation nanoelectronics, 2D SnSe is anticipated to possess attractive electronic and optoelectronic properties, such as thickness-dependent bandgap and high photoresponse. In this context, to facilitate the exploration of functional properties and applications of 2D SnSe, it is crucial to develop controllable synthesis routes that yield large-area, ultrathin, and high-quality SnSe crystals.

In this work, we demonstrate the growth of 2D SnSe crystals on mica via a low-pressure physical vapor deposition (PVD) method (Figure 1); the crystals display in-plane ferroelectricity that is confirmed using polarization-dependent reflectivity spectroscopy.

Effects of substrate pre-annealing, temperature, pressure, and growth time on the lateral size and thickness of as-grown SnSe are further systematically studied, enabling us to rationally optimize the growth parameters to obtain large ultrathin SnSe. Growth temperature and pressure are identified as crucial factors for tuning the ultimate size and thickness of SnSe crystals because they can largely affect the precursor evaporation, diffusion, and deposition processes. Besides, we find that air-annealing of mica at 400 °C before the growth process can lead to SnSe crystals with increased lateral sizes. Under optimized growth conditions, 2D SnSe crystals with lateral size up to ~23.0 μm and controllable thicknesses down to ~2.0 nm (3-4 layers) are achieved. Our work takes a significant step forward on the large-scale controllable synthesis of 2D SnSe, facilitating the investigation of its thickness-dependent properties and related applications.



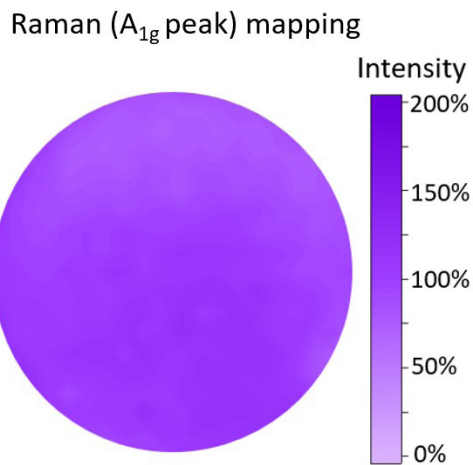
▲ Figure 1: Controlled synthesis of 2D SnSe crystals. (a) Schematic illustration of low-pressure PVD setup for SnSe synthesis. (b) Typical optical microscopy image of as-synthesized SnSe crystals on mica. (Inset: top view of the crystal structure of orthorhombic SnSe). (c) Optimized growth conditions for synthesizing large-sized ultrathin SnSe crystals (5.0 nm thin with a lateral size of 23.0 μm) and a corresponding atomic force microscopy image.

Low-temperature Synthesis of Monolayer MoS₂ on 200-mm Silicon Platform

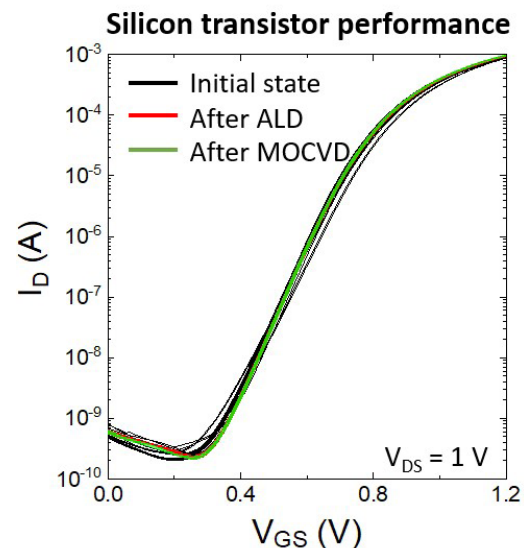
J. Zhu, J.-H. Park, M. Mohamed, T. Zhang, M. Xue, J. Kong, T. Palacios
Sponsorship: Ericsson, Semiconductor Research Corporation (SRC)

The emerging 2D materials have attracted great attention in the past decade and are being considered as promising candidates for the next-generation heterogeneous electronic and photonic systems. There have also been many demonstrations of wafer-scale synthesis, e.g., 2-inch or 4-inch, of monolayer MoS₂. However, these chemical vapor deposition (CVD) or metal-organic chemical vapor deposition (MOCVD) methods require high growth temperature (> 600°C), which is not compatible with silicon back-end-of-line (BEOL) integration unless an additional wafer-scale transfer process is used. This makes the heterogeneous integration of 2D materials and silicon very difficult.

In this work, we demonstrate, for the first time, 8-inch MoS₂ monolayer thin film grown at 250°C by the MOCVD method. The short growth time (40-70 mins), in combination with the low thermal budget, allows direct silicon BEOL-compatible integration without any transfer process. The synthesized MoS₂ demonstrates good wafer-level uniformity (Figure 1) and does not degrade the silicon transistors underneath (Figure 2). This novel low-temperature synthesis method paves the way for heterogeneous integration of 2D materials with silicon circuits, allowing the higher-density integration needed in the next-generation of electronics, e.g., Internet-of-Things applications.



▲ Figure 1: Measured Raman mapping (A_{1g} peak) over the 8-inch wafer. Excellent material uniformity can be observed.



▲ Figure 2: Measured transfer characteristics of: (black lines) 10 as-fabricated silicon transistors, (red line) 1 silicon transistor after depositing 20-nm Al₂O₃ by using a commercial ALD (250°C, 57 min.) and (green line) 1 silicon transistor after depositing monolayer MoS₂ thin film using our new MOCVD growth process (250°C, 60 min.).

FURTHER READING

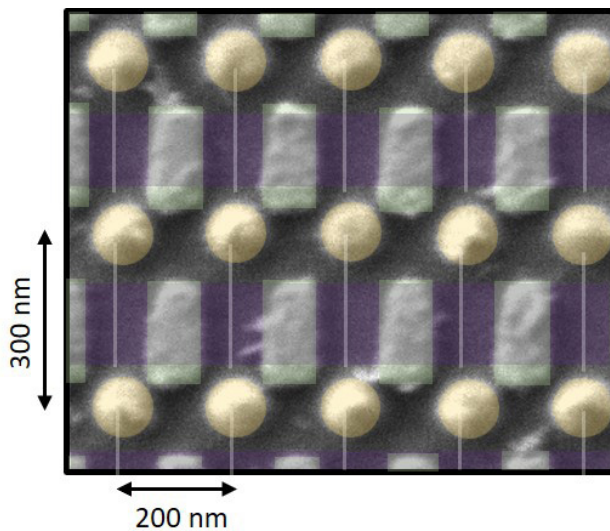
- H. Wang, L. Yu, Y.-H. Lee, Y. Shi, A. Hsu, M. L. Chin, L.-J. Li, M. Dubey, J. Kong, and T. Palacios, "Integrated Circuits Based on Bilayer MoS₂ Transistors," *Nano Letters*, vol. 12, pp. 4674-4680, 2012.
- L. Yu, D. El-Damak, U. Radhakrishna, X. Ling, A. Zubair, Y. Lin, Y. Zhang, M.-H. Chuang, Y.-H. Lee, D. Antoniadis, J. Kong, A. Chandrakasan, and T. Palacios, "Design, Modeling, and Fabrication of Chemical Vapor Deposition Grown MoS₂ Circuits with E-Mode FETs for Large-Area Electronics," *Nano Letters*, vol. 16, pp. 6349-6356, 2016.
- M.-Y. Li, S.-K. Su, H.-S. P. Wong, and L.-J. Li, "How 2D Semiconductors Could Extend Moore's Law," *Nature*, vol. 567, pp. 169-170, 2019.

Carbon Nanotube Nano-contacts for MoS₂ Transistors

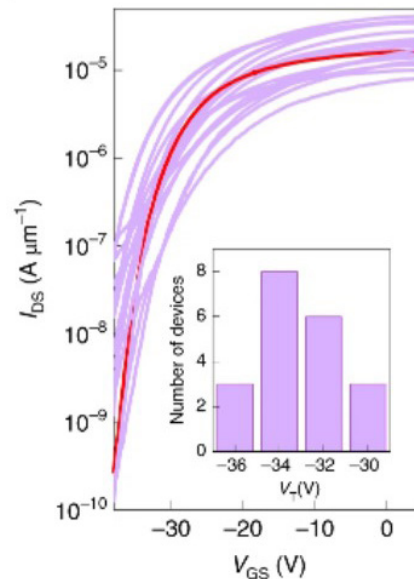
J. Zhu, Y. Guo, E. Shi, J.-H. Park, J. Kong, T. Palacios
Sponsorship: Institute of Soldier Nanotechnologies (ISN)

With the scaling of electronic devices, the contact length is also shrinking rapidly and is about 20 nm in the most advanced silicon technology nodes. Further scaling of contact length will be difficult as the electron scattering from the grain boundaries and sidewalls of the metal contacts will be more and more significant, increasing the resistance of the metal contacts and also degrading the contact quality. Carbon nanotubes (CNTs), however, possess smooth surfaces and nanometer-scale diameter and avoid grain boundary scattering thanks to their long aspect ratio. All these properties make CNTs promising candidates for future nanoscale contacts.

In this work, we demonstrate, for the first time, MoS₂ transistors with CNT bundles as the source/drain contacts. By using super-aligned CNT bundles, we fabricated a high-density 8x8 array of MoS₂ transistors with single device area of ~ 0.06 μm² (Figure 1). The clean van der Waals interface between CNTs and MoS₂ allows the CNT bundles to demonstrate a very low contact resistance ~2.0 kΩ·μm (the lowest being 1.6 kΩ·μm), which is comparable to the one in graphene contacts and even better than most of the conventional metal contacts, e.g., Au or Ni. This low contact resistance allows the device to show excellent electrical performance, which makes them ideal for highly scaled electronics.



▲ Figure 1: False color scanning electron microscope image of eight local top-gate transistors in a 2D MoS₂ transistor array with single device area of 0.06 μm². Green rectangles are the local top gates. Dark yellow/orange circles are the vertical metal-filled via in contact with the CNT bundles (white lines). Purple rectangles are monolayer MoS₂ channels. 10-nm Al₂O₃ is used as the top-gate dielectric. (Guo 2022).



▲ Figure 2: Measured transfer characteristics of 20 MoS₂ transistors with CNT bundle contacts at room temperature and V_{DS} = 1V. The red line demonstrates the representative performance among the 20 devices; inset, threshold voltage (V_T) distribution of the 20 devices. (Guo 2022).

FURTHER READING

- Y. Guo†, E. Shi†, J. Zhu†, P.-C. Shen, J. Wang, Y. Lin, Y. Mao, S. Deng, B. Li, J.-H. Park, A.-Y. Lu, S. Zhang, Q. Ji, Z. Li, C. Qiu, S. Qiu, Q. Li, L. Dou, Y. Wu, J. Zhang, T. Palacios, A. Cao, and J. Kong, "Soft-lock Drawing of Super-aligned Carbon Nanotube Bundles for Nanometer Electrical Contacts," *Nature Nanotechnology*, vol. 17, pp. 278-284, 2022.
- H. Wang, L. Yu, Y.-H. Lee, Y. Shi, A. Hsu, M. L. Chin, L.-J. Li, M. Dubey, J. Kong, and T. Palacios, "Integrated Circuits Based on Bilayer MoS₂ Transistors," *Nano Letts*, vol. 12, pp. 4674-4680, 2012.
- L. Yu, D El-Damak, U. Radhakrishna, X. Ling, A. Zubair, Y. Lin, Y. Zhang, M.-H. Chuang, Y.-H. Lee, D. Antoniadis, J. Kong, A. Chandrakasan, and T. Palacios, "Design, Modeling, and Fabrication of Chemical Vapor Deposition Grown MoS₂ Circuits with E-Mode FETs for Large-Area Electronics," *Nano Letts*, vol. 16, pp. 6349-6356, 2016.